volume varies from 0.3 to 1.0. The dependence of gas permeability on ply angle of the carbon cloth is also examined. The permeability for the case of 90-deg ply angle is about three times larger than that for the case of 0-deg ply angle. It is also shown that the variation of the measured permeability in terms of ply angle can be fitted fairly well with the curve determined by Eq. (4). In the study of delamination problem, thermal response of ablative test piece should be solved at least in two-dimensional space. The dependence of gas permeability on ply angle that is measured in this study will be used in such studies.

References

[1]Yamada, T., Ishii, N., Inatani, Y., and Honda, M., "Thermal Protection System of the Reentry Capsule with Superorbital Velocity," Inst. of Space and Astronautical Science, Rept. SP No. 17, Sagamihara, Japan, March 2003, pp. 245–261.

[2]Potts, R. L., "Application of Integral Methods to Ablation Charring Erosion, A Review," *Journal of Spacecraft and Rockets*, Vol. 32, No. 2, 1995, pp. 200–209.

[3]Ahn, H.-K., Park, C., and Sawada, K., "Response of Heatshield Material at Stagnation Point of Pioneer-Venus Probe," *Journal of Thermophysics and Heat Transfer*, Vol. 16, No. 3, 2002, pp. 432–439.

[4]McManus, H. L., "High-Temperature Thermochemical Behavior of Carbon–Phenolic and Carbon–Carbon Composites," Ph.D. Dissertation, Dept. of Mechanical Engineering, Stanford Univ., Stanford, CA, 1990.

[5]McManus, H. L., and Springer, G. S., "High Temperature Thermochemical Behavior of Carbon–Phenolic and Carbon–Carbon Composites, II. Results," *Journal of Composite Materials*, Vol. 26, No. 2, 1992, pp. 230–255.

Vibrational Population Enhancement in Nonequilibrium Dissociating Hypersonic Nozzle Flows

Eswar Josyula*
U.S. Air Force Research Laboratory, Wright–Patterson Air Force Base, Ohio 45433
and
William F. Bailey†
U.S. Air Force Institute of Technology, Wright–Patterson Air Force Base, Ohio 45433

Nomenclature

K_{eq} = equilibrium constant
k_f = dissociation-rate coefficient
k_r = recombination-rate coefficient
p = pressure
T = translational temperature
T_u = vibrational temperature
α_O = mass fraction of atomic oxygen
Θ_d = characteristic temperature of dissociation
ρ = total density
ρ_i = state density in the ith vibrational level
ρ_n = state density in the nth vibrational level
φ_n = depletion factor for state n, deviation of quasisteady distribution from equilibrium Boltzmann $\rho_n = \rho_n^o(1 + \varphi_n)$

Presented as Paper 2003-3778 at the AIAA 36th Thermophysics Conference, Orlando, FL, 23 June 2003; received 27 January 2004; revision received 3 May 2004; accepted for publication 3 May 2004.

*Research Aerospace Engineer, AFRL/VAAC, 2210 Eighth Street. Associate Fellow AIAA.

†Associate Professor, AFIT/ENP, 2950 Hobson Way.

Introduction

THE proper treatment of energy transfer between nonequilibrium molecular energy modes and dissociation has important implications in the accurate prediction of the aerothermodynamics of gas systems, namely, aerodynamic heating on hypersonic vehicles and thrust in propulsive nozzles.[1] At high temperatures, molecular collisions result in the exchange of the translational, rotational, vibrational, and electronic energies of the collision partners. The probabilities or effective cross sections of these elementary processes differ significantly, giving rise to widely separate relaxation times for the internal modes. Thus it becomes important to account for the rates of relaxation processes to predict the nonequilibrium behavior of these kinds of flows. Vibrational equilibration involves widely separated relaxation times ranging between the very short times for translational/rotational equilibration and the longer times for chemical and ionization equilibration. The disparate eigenvalues have significant physical and computational implications. Nonequilibrium vibrational energy distributions are required for prediction of dissociation rates, interpretation of radiation experiments, and interpretation of ionic recombination rates.

The effect of vibrational population depletion in dissociating flows behind shock waves for hypersonic applications was presented in the work of Josyula and Bailey.[2] The collisional approach to dissociation was adapted to model the nonequilibrium flow physics in the study of the dissociation kinetics of hypersonic flow past a blunt body. In this study, the vibrational master equations were coupled to fluid dynamic equations, and vibration-translation (V-T) process were considered in evaluating the vibrational population depletion effects of dissociation from the last quantum level. The role of the V-T process in the dissociation kinetics was delineated by assessing the competition between the V-T process, which primarily restores equilibrium, and the dissociation process, which perturbs the equilibrium state. The extent of the population depletion and the consequent reduction of the dissociation rates is sensitive to the temperature regime in the flowfield. For the dissociation kinetics of the nitrogen molecule, in the temperature range of 5000–15,000 K the new vibration-dissociation model yielded a substantial rate reduction relative to Park's equilibrium rate. The nonequilibrium conditions behind the shock wave of a blunt body exemplify the case where the translational temperature is greater than the vibrational temperature ($T > T_v$), ultimately approaching near-equilibrium conditions close to the surface of the body. The higher rate of dissociation vs recombination in blunt-body flows makes the vibrational population depletion effect significant in the vibration-dissociation coupling model.

In expanding nozzle flows, however, the effect of vibration-dissociation coupling on the vibrational population density is reversed and the population is enhanced. The sonic flow at the throat of the nozzle is in thermal equilibrium, and as the flow proceeds towards the exit of the nozzle the flow departs from the equilibrium conditions. The vibrational temperature freezes near the throat, and the translation temperature rapidly falls as a result of the expansion process. The flow exhibits higher degrees of nonequilibrium as it proceeds towards the exit. As the translational temperature starts dropping, the dissociation rate drops significantly. However for the same translational temperature drop, the change in the recombination rate is small, and the recombination rate remains consistently higher than the dissociation rate throughout most of the nozzle flowfield. This recombination-dominant flow leads to a population enhancement in the vibrational manifold under the nonequilibrium reactive conditions. A vibration-dissociation coupling model, thus, has to account for this enhancement to accurately predict the nonequilibrium chemistry. The role of the vibrational population enhancement in the development of vibration-dissociation coupling model in high-temperature nozzle flows in hypersonic applications is the objective of the present study.

The nonequilibrium vibrational energy distribution was modeled by the master equations to calculate the population distributions by

considering the kinetics of particle exchanges among the quantum states. The flow in a high-temperature nozzle flow of oxygen is considered for a high temperature of 5000 K at the nozzle throat, where significant dissociation requires both reactive and nonreactive kinetics processes be included. The fluid dynamic equations coupled to the master equations including the V-T, vibration-vibration (V-V), dissociation, and recombination effects were solved to delineate the various kinetic processes occurring in the nozzle, with the objective of refining the just-mentioned vibration-dissociation coupling model. Further details of the models are found in Ref. 3.

To discuss the contrasting effects on the vibrational population, the vibration-dissociation coupling model presented in the earlier study[4] is briefly described. The vibration-dissociation coupling model with depletion effects presented in the earlier study solved the generalized depletion equation. The analysis introduced a parameter φ to characterize the deviation of the perturbed quasisteady distribution from an equilibrium Boltzmann distribution. That is, if the equilibrium distribution is denoted by ρ_n^o and the quasisteady distribution by $\rho_n(t)$, then $\rho_n(t) = \rho_n^o(1+\varphi_n)$. It is seen that when $\varphi < 0$ the level population decreases relative to the equilibrium population. The generalized depletion equation of the vibration-dissociation coupling model with the parameter φ for V-T and V-V systems was presented in the earlier paper.

The preceding analysis applies to dissociation-dominant flows where the translational temperature is high, vibrational temperature is low, and the vibrational modes are heated in the convective process, such as in the flow past blunt body. In expanding nozzle flows, however, the vibrational temperature freezes at a relatively high temperature compared to the translational temperature, and the recombination-dominant, nonequilibrium reactive flow enhances the population in the vibrational manifold from its equilibrium distribution.

Figure 1 shows the dissociation k_d and the recombination coefficient k_r, with the following definitions. For the dissociation reaction,

$$k_f = C_f T^{\eta} \exp(-\Theta_d/T) \exp(-\Theta_d/T) \tag{1}$$

where C_f and η are from experiments taken from the work of Park.[5] Under nonequilibrium conditions, the temperature T in the preceding equation is an effective temperature based on the translational and internal energy modes. This effective temperature is commonly calculated in today's hypersonic computational-fluid-dynamics codes by the empirical two-temperature dissociation model attributed to Park. The goal of the present numerical study is to perform a state-to-state kinetic modeling of the nonequilibrium flow physics for developing physically meaningful vibration-dissociation coupling models. The atom recombination rate is obtained from

$$k_r = k_f / K_{\text{eq}} \tag{2}$$

where K_{eq} is the equilibrium constant determined from curve fits[5] of experimental data. As the temperature drops, the dissociation rate decreases, and the recombination rate increases with temperature. This figure is discussed further in the Results section.

An expanding nozzle flow of oxygen was modeled to study the effect of vibrational and reactive kinetics on the flowfield. The expanding nozzle flow provides an excellent test bed to study the new vibration-dissociation model, simulated also by Shizgal and Lordet.[6] The nozzle with a throat radius of 3 mm has an area ratio of 50. For the reacting case, a higher throat temperature of 5000 K with 0.3376 oxygen atom mass fraction and $p_{\text{throat}} = 9479$ kPa was specified. The static pressure at throat is 9479 kPa. The numerical algorithm employed to solve the coupled set of equations is the Roe flux difference method described in Ref. 7.

Results and Discussion

The translational and vibrational temperatures along the length of the nozzle (Fig. 2) show that the vibrational temperature along the length of the nozzle reduces at a slower rate than the translational temperature. Note that the V-T transfers take place in a gas where the vibrational temperature is higher than the translational temperature. Because the translational temperature decreases very rapidly in an expanding nozzle, the dissociation rates fall sharply, and recombination of atoms increases along the length of the nozzle. Resulting mass fraction of the O_2 and O species along the length of the nozzle is shown in Fig. 3. The highest gas temperature under equilibrium conditions exist at the throat of the nozzle. Downstream of the nozzle, the lower dissociation rates and a faster decrease of the total density (at the lower temperatures) cause the O_2 mass fraction to increase and are greater than the equilibrium throat value at the rear of the nozzle. Correspondingly, the oxygen-atom mass fraction drops along the length of the nozzle.

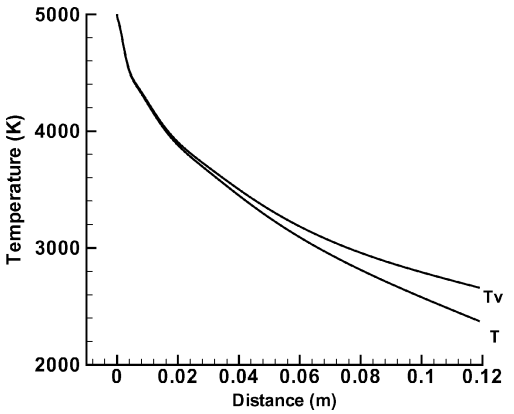

Fig. 2 Translational and vibrational temperatures along length of nozzle: $T_{\text{throat}} = 5000$ K, $p_{\text{throat}} = 9479$ kPa, medium = O_2, $\alpha_O = 0.3376$.

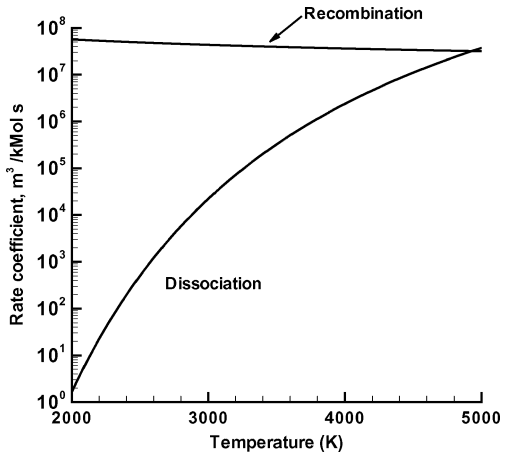

Fig. 1 Dissociation and recombination rate for the $O_2 + O_2 = 2O + O_2$ reaction.

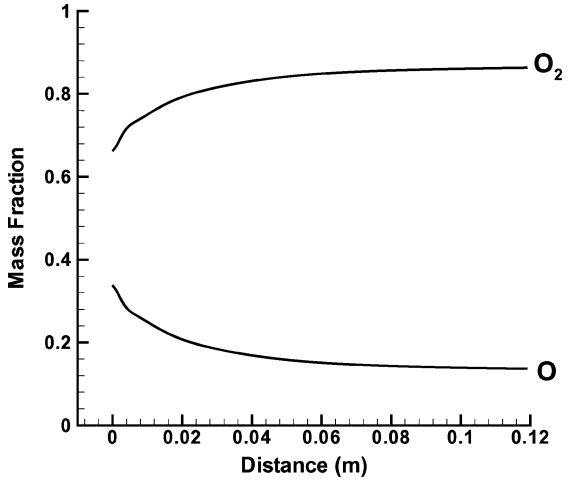

Fig. 3 Mass fraction along length of nozzle: $T_{\text{throat}} = 5000$ K, $p_{\text{throat}} = 9479$ kPa, medium = O_2, $\alpha_O = 0.3376$.

Table 1 Nozzle locations and flow conditions for which population enhancements demonstrated

Location	Distance from throat, m	T, K	T_v, K	O_2 mass fraction	Density, kg/m^3	Enhancement factor from Boltzmann in last level
Near throat	0.02	3851	3876	0.796	0.641	1.15
At exit	0.1	2548	2761	0.862	0.0622	120

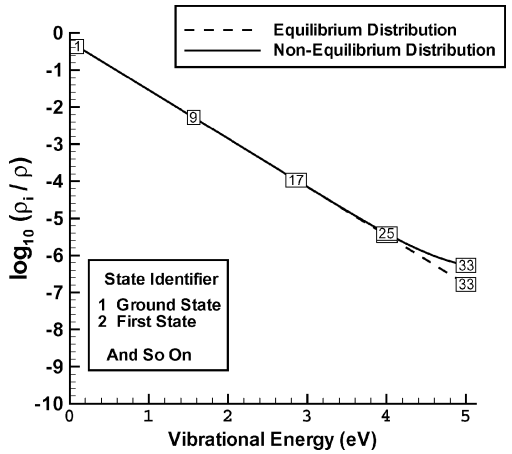

Fig. 4 Population distribution near nozzle throat: $T_{\text{throat}} = 5000$ K, $p_{\text{throat}} = 9479$ kPa, medium = O_2, $\alpha_O = 0.3376$.

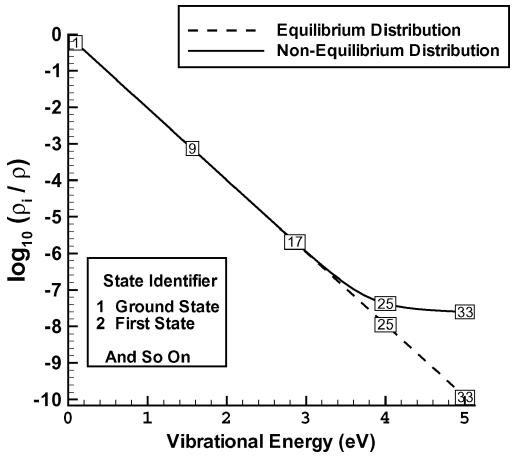

Fig. 5 Population distribution near nozzle exit: $T_{\text{throat}} = 5000$ K, $p_{\text{throat}} = 9479$ kPa, medium = O_2, $\alpha_O = 0.3376$.

The vibrational population enhancement in nonequilibrium nozzle flows is demonstrated in Figs. 4 and 5. Results are shown at two nozzle locations: 1) close to the throat at a distance of 0.02 m from throat and 2) at the exit of nozzle. The population distributions corresponding to the Boltzmann are compared to the nonequilibrium populations obtained from solving the master equations accounting for vibrational and dissociation kinetics. The translational temperature and the density are highest near the nozzle throat and fall along the nozzle. The O mass fraction decreases, and the O_2 mass fraction increases along the nozzle, signifying atom recombination (see Fig. 3). The nozzle flow details for the two locations are shown in Table 1. The nonequilibrium population distributions shown in Figs. 4 and 5 demonstrate an enhancement at both locations of the nozzle. Compared to a Boltzmann distribution, near the throat, Fig. 4, the nonequilibrium population enhancement in the last level is a factor of 1.15. The population enhancement increases downstream of the nozzle, with factor of 120 near the exit (Fig. 5). The quantitative assessment of the population enhancement as a result of atom recombination is useful in calculating the nonequilibrium dissociation and recombination rates of a chemical reaction from its equilibrium rates in hypersonic expanding nozzle flows.

The effect of population enhancement is to lower the effective recombination rate. Even without the consideration of the effects of the population enhancement on the dissociation rates, the temperature drop along the nozzle has the effect of reducing the dissociation rates. However, the effect of population enhancement is to lower this reduction. In other words, with temperatures decreasing along the nozzle the population enhancement lowers the disparity between the dissociation and recombination rates.

At the throat of the nozzle, the equilibrium temperatures prevail. As the temperature decreases downstream, the effect of the population enhancement is to adjust the rate of dissociation and recombination by lowering the mass fraction of O_2 and increasing that of O along the nozzle. From the figure shown earlier for the dissociation and recombination rates (Fig. 1), it is seen that when the temperature drops from 5000 to 3000 K the recombination-rate coefficient is nearly the same. For the same temperature drop, the fall in the dissociation-rate coefficient is significant and decreases by a factor of about 1700. Also, the recombination-rate coefficient is higher than the dissociation rate downstream of the throat. For this recombination-dominant flow, the calculations of the vibrational population enhancement demonstrated in the present study provide a useful relationship to calculate the effective nonequilibrium dissociation and recombination rates from the equilibrium rates.

Conclusions

A computational study was conducted for hypersonic expanding nozzle flows of oxygen to define the role of vibrational population enhancement in the development of vibration-dissociation coupling model. For the reacting gas case, the higher atom-recombination rate compared to the dissociation rate was found to be responsible for the vibrational population enhancement downstream of the nozzle. For use in the development of vibration-dissociation coupling models, the physics of these recombination-dominant flows is contrasted to dissociation-dominant flows, typically, encountered behind shock waves. Behind shock waves, the vibrational population is depleted as a result of dissociation where the coupling simulates the competition between the dominant vibration-translation processes (compared to V-V), which primarily restore equilibrium and the dissociation processes involving the molecular transitions to the continuous vibrational state that perturb the equilibrium state. In nozzle flows, however, the vibrational population is enhanced downstream of the nozzle as a result of the higher atom recombination. The population enhancement in nozzle flows leads to a reduction of the effective recombination rate. Both population depletion and enhancement play a crucial role in the vibration-dissociation coupling models used in hypersonic computational-fluid-dynamics codes.

References

[1]Rich, J. W., Macheret, S. O., and Adamovich, I. V., "Aerothermodynamics of Vibrationally Nonequilibrium Gases," *Experimental Thermal and Fluid Science*, Vol. 13, No. 1, 1996, pp. 1–10.

[2]Josyula, E., and Bailey, W. F., "Vibration-Dissociation Coupling Using Master Equations in Nonequilibrium Hypersonic Blunt-Body Flow," *Journal of Thermophysics and Heat Transfer*, Vol. 15, No. 2, 2001, pp. 157–167.

[3]Josyula, E., and Bailey, W. F., "Vibrational Population Enhancement in Nonequilibrium Hypersonic Nozzle Flows," AIAA Paper 2003-3778, June 2003.

[4]Josyula, E., and Bailey, W. F., "Vibrational Relaxation and Population Depletion of Nitrogen in Hypersonic Flows," AIAA Paper 2002-0200, Jan. 2002.

[5]Park, C., "A Review of Reaction Rates in High Temperature Air," AIAA Paper 89-1740, June 1989.

[6]Shizgal, B. D., and Lordet, F., "Vibrational Nonequilibrium in a Supersonic Expansion with Reaction: Application to O_2-O," *Journal of Chemical Physics*, Vol. 104, No. 10, 1996, pp. 3579–3597.

[7]Josyula, E., "Computational Study of Vibrationally Relaxing Gas Past Blunt Body in Hypersonic Flows," *Journal of Thermophysics and Heat Transfer*, Vol. 14, No. 1, 2000, pp. 18–26.

View-Factor-Based Radiation Transport in a Hypersonic Shock Layer

Deepak Bose* and Michael J. Wright†
NASA Ames Research Center,
Moffett Field, California 94035

Introduction

ATOMS and molecules in the hot shock layer formed in front of a hypersonic vehicle often release some of their internal energy by spontaneous emission of electromagnetic radiation. The isotropically emitted radiative energy propagates through the shock layer, sometimes undergoing absorption, until a portion of the remaining energy eventually reaches the body surface and heats the vehicle. In cases of high-speed entries of large vehicles, the radiative heating can be larger than the convective heating from the hot gas. It is therefore crucial to the design of the protective heat shield that this radiative-transport process be modeled accurately.

In practice radiative transport is typically reduced to a one-dimensional line-of-sight problem by assuming small body curvature and small tangential flow gradients. This approach is known as the tangent slab model. In this Note, we present a three-dimensional transport model based on geometric view factors between the emitting volumes and surface elements, which significantly improves the accuracy of radiative heat-flux estimates for an optically thin shock layer. This method can also be applied to absorbing gases, but the cost can be significantly more than the tangent slab model if fine spectral resolution is required.

Methodology

Shocklayer radiation is usually computed by assuming that it is uncoupled from the fluid dynamics. In this approach, the flowfield around the vehicle body is first simulated on a computational grid using a computational fluid dynamics (CFD) technique. The emission intensity $I_i(\nu)\,\mathrm{d}\nu$ W/m^3, where ν is the emission frequency, is then obtained at each computational cell i using known species densities and temperatures. The intensity can be computed using a full line-by-line method[1] or by using approximate band models. Assuming isotropic propagation, the radiative heat flux as a result of emission from the computational cell i with volume ΔV_i, to a surface element j with surface area ΔA_j (see Fig. 1) is written as[2]

$$\Delta q_{ij} = b_{ij} \int \frac{I_i(\nu)\Delta V_i}{\Delta A_j}\left(\frac{\Delta A_j \cos\theta_{ij}}{4\pi r_{ij}^2}\right)\tau(r_{ij},\nu)\,\mathrm{d}\nu \qquad (1)$$

where r_{ij} is defined in Fig. 1 as the distance between the center of the emitting volume and the center of the target area and θ_{ij} is the angle between the line of sight and the surface normal. The term

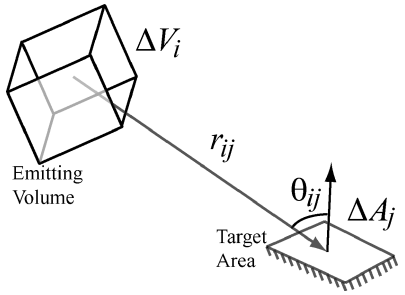

Fig. 1 Schematic of the line of sight and the relevant angle used in the view factor definition.

$\tau(r_{ij},\nu)$ is the attenuation factor caused by absorption in the gas and assumes a value of one for the optically thin case. The binary operator b_{ij} accounts for shadowing (caused by obstruction) effects that can arise for bodies with concave curvature; $b_{ij}=0$ if the line of sight intersects another portion of the surface prior to intersecting the target element and $b_{ij}=1$ otherwise. The computation of shadowing greatly increases the cost of the view factor algorithm and is not necessary for convex bodies. The areas on the back side of a convex body that does not see the radiation are eliminated as target elements because of a negative view factor ($\cos\theta_{Ij}<0$). Therefore, the binary operator b_{ij} is used only when a portion of the vehicle has a concave curvature, for example, vehicles with control surfaces.

The geometric view factor, defined as[2] $\Delta A_j \cos\theta_{ij}/4\pi r_{ij}^2$, is the fraction of radiative power that reaches the target surface element in the absence of absorption. The total radiative heat flux on surface element j is computed by summing over all emitting volumes:

$$q_j = \sum_i \Delta q_{ij} \qquad (2)$$

The validity of Eq. (1) rests on the assumption that dimensions of the emitting volume and the target area are much smaller than the distance between them. However, this condition is frequently violated in typical flowfield simulations because the thickness of the hot emitting layer between the shock and the body can be small enough that the cell dimensions are comparable to this thickness. Simply using Eq. (1) in such a case can yield unrealistically large view factors. This suggests that further refinement of the CFD grid is needed to compute the radiative transport. Therefore we divide the computational cells and the surface elements into smaller equal sized subcells. Each of these subcells has the same unit intensity as the original, but the view factors are different. If the emitting cell i is divided into m_0 subcells and the target surface element j into n_0 subelements, the modified radiative heat flux can be written as

$$\Delta q_{ij} = b_{ij} \int I_i(\nu)\frac{\Delta V_i}{\Delta A_j}\frac{1}{n_0 m_0}\sum_{m,n}\left(\frac{\Delta A_j \cos\theta_{imjn}}{4\pi r_{imjn}^2}\right)\tau(r_{imjn},\nu)\,\mathrm{d}\nu \qquad (3)$$

Strictly speaking, the number of subcells must be large enough to ensure that the resulting cell dimensions are much smaller than r_{ij}. However, near-wall cells (small r_{ij}), which would require the most subdivisions, are typically weakly emitting and do not contribute significantly to the radiative heating. Therefore in practice the cells are subdivided only until the change in predicted radiative heating is small.

Spherical-Cap Shock Layer

As an example, an analytical solution for radiative transport can be obtained for an optically thin hemispherical shock layer formed over a hemispherical body, as shown in Fig. 2. First, if we assume that radiation intensity I is constant over the shock layer of thickness Δr, we obtain the radiative heat flux at the stagnation point by integrating over the shock layer using the view factors to be

$$q_{\mathrm{vf}} = (I\Delta r/2)\left[\left(1-\sqrt{1-\beta^2}\right)/\beta^2\right], \qquad \beta = r_b/r_s \qquad (4)$$

Received 5 March 2004; revision received 4 June 2004; accepted for publication 7 June 2004.

*Senior Research Scientist, ELORET Corporation, Mail Stop 230-3. Member AIAA.

†Senior Research Scientist, Reacting Flow Environments Branch. Senior Member AIAA.